Parametric Study of State of Charge for an Electric Aircraft in Urban Air Mobility

Priyank Pradeep *
Universities Space Research Association, NASA Ames Research Center, Moffett Field, CA, 94035, USA.

Chetan S. Kulkarni †
KBR Wyle Services, LLC, NASA Ames Research Center, Moffett Field, CA, 94035, USA.

Gano B. Chatterji ‡
Crown Consulting Inc., NASA Ames Research Center, Moffett Field, CA, 94035, USA.

Todd A. Lauderdale §
NASA Ames Research Center, Moffett Field, CA, 94035, USA.

A parametric study of the state of charge is performed using two separate battery models, i.e., energy-based and electrochemical-based battery models for a NASA-proposed conceptual multirotor aircraft in the urban environment. The parametric study is performed using an optimal control framework. The parameters considered for the parametric analysis are cruise airspeed, cruise altitude, climb profile, range, and required time of arrival under uncertainties (wind and departure-time). The key results suggest: i) the minimum-energy cruise airspeed (maximum final state of charge) increases with an increase in cruise altitude, ii) the minimum-energy cruise airspeed is independent of range; iii) design a cruise corridor for urban air mobility air traffic at the lowest possible altitude considering eddies/vortices from skyscrapers, other types of air traffic, and vertical obstacles, and iv) wind and departure-time uncertainties could adversely impact the predictability of the usage of the onboard lithium-ion polymer battery pack for an aircraft flying to meet the assigned required time of arrival in the urban air mobility environment. The state of charge results showed high dependence on the battery model. Therefore, this study demonstrates the need to have a validated battery model for the onboard lithium-ion polymer battery pack to predict the state of charge accurately.

I. Nomenclature

λ	=	Latitude of the aircraft
τ	=	Longitude of the aircraft
h	=	Altitude above mean sea level of the aircraft
m	=	Mass of the aircraft
V	=	True airspeed of the aircraft
V_l	=	Lateral component of the true airspeed of the aircraft
V_v	=	Vertical component of the true airspeed of the aircraft
V_{GS}	=	Groundspeed of the aircraft
γ	=	Aerodynamic flight path angle of the aircraft
ψ	=	Heading angle of the aircraft
χ	=	Course angle of the aircraft
D	=	Parasite drag on the aircraft
T	=	Net thrust
n	=	Number of rotors installed on the aircraft

*Aerospace Engineer, Universities Space Research Association, NASA Ames Research Center, AIAA Senior Member.
†Research Scientist, KBR Wyle Services, LLC, NASA Ames Research Center, AIAA Associate Fellow.
‡Senior Scientist and Lead, Crown Consulting Inc., NASA Ames Research Center, AIAA Associate Fellow.
§Aerospace Engineer, Aviation Systems Division, NASA Ames Research Center.

α	=	Angle of attack of air-stream relative to rotor tip-path-plane
θ	=	Rotor tip-path-plane pitch angle
ϕ	=	Rotor tip-path-plane roll angle
κ	=	Induced power factor
ω	=	Rotational speed of the rotor blades
σ	=	Thrust weighted solidity ratio
$C_{\text{d mean}}$	=	Mean blade drag coefficient
A_{rotor}	=	Rotor disk area
R	=	Radius of the rotor
v_h	=	Rotor induced velocity in hover
v_i	=	Rotor induced velocity during forward flight
T_{rotor}	=	Thrust produced by an isolated rotor
C_{T}	=	Rotor Thrust coefficient
I_i	=	Moment of inertia of the i^{th} rotor
P_{max}	=	Total maximum deliverable power
P_{req}	=	Instantaneous power required in forward flight
P_{battery}	=	Instantaneous power supplied by the onboard lithium-ion polymer battery pack
ρ	=	Density of air
R_{Earth}	=	Radius of the Earth assuming spherical model
W_e	=	East component of wind velocity
W_n	=	North component of wind velocity
W_v	=	Vertical (up) component of wind velocity
DEP	=	Distributed electric propulsion
EOD	=	End-of-discharge of the onboard lithium-ion polymer battery pack
EVTOL	=	Electric vertical takeoff and landing
Li-Po	=	Lithium-ion polymer battery
RTA	=	Required time of arrival
SOC	=	State of charge of the onboard lithium-ion polymer battery pack
STD	=	Scheduled time of departure
UAM	=	Urban air mobility
UTM	=	Unmanned aircraft system traffic management
V(t)	=	Voltage of the onboard lithium-ion polymer battery pack
V_{MO}	=	Maximum operating limit airspeed

II. Introduction

The envisioned concept of urban air mobility (UAM) is anticipated to support passenger transportation, cargo delivery, and emergency services in major metropolitan areas with increasing autonomy levels in the future [1, 2]. Distributed electric propulsion powered electric vertical takeoff and landing (eVTOL) aircraft are expected to enable urban air mobility [1]. Recently, technological advances have made it possible to build and flight test eVTOL aircraft [2]. Several companies, for example, Airbus A^3, Aurora Flight Sciences, EHang, Joby Aviation, Kitty Hawk, Leonardo, Lilium, Terrafugia, and Volocopter, are pursuing different design approaches to make eVTOLs a reality [2]. Despite various designs, they all have distributed electric propulsion (DEP) systems in common [3]. However, the low specific energy of current lithium-ion polymer (Li-Po) battery technology used in DEP imposes constraints on the flight endurance of such aircraft. Therefore, to enable autonomous urban air mobility operations using electric aircraft, one of the critical steps from a safety perspective is to accurately and periodically predict whether the current state of the onboard Li-Po battery pack is sufficient to support the flight mission under given operational and environmental conditions with an adequate safety margin [4, 5]. On the other hand, from an efficiency perspective a key step is to understand the most energy-efficient flight profile (cruise airspeed, cruise altitude, climb, and descent profiles). The operational benefits of optimizing altitude and speed profiles for fuel, noise, time, and direct operating cost have been extensively studied for commercial aircraft and rotorcraft but not for eVTOLs in the UAM environment [3, 6–8]. Therefore, the primary motivation of the paper is to understand the impact of various operational and environmental parameters on the state of the onboard Li-Po battery pack of the aircraft in the urban environment [1, 9]. In this research, for parametric study of the state of the onboard Li-Po battery pack: i) state of charge (SOC) has been considered as a

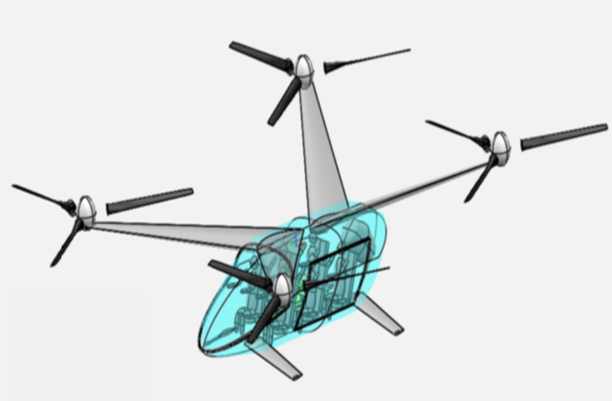

(a) Quadrotor eVTOL aircraft [10]

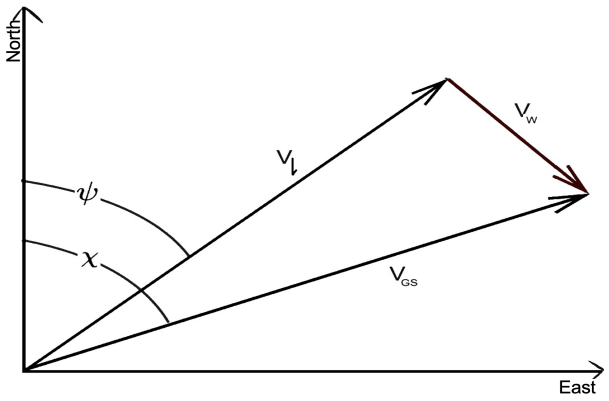

(b) Lateral navigation definition [6]

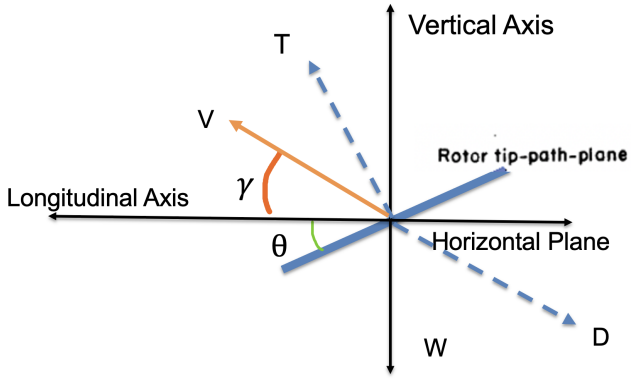

(c) Rotor tip-path-plane pitch angle definition [3]

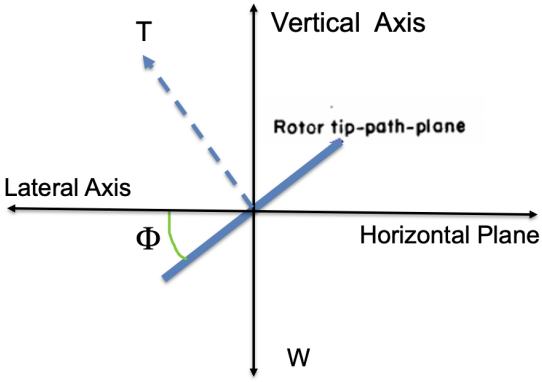

(d) Rotor tip-path-plane roll angle definition [6]

Fig. 1 Multirotor eVTOL aircraft in forward flight

metric equivalent to the fuel gauge of the electric fuel system and ii) cruise airspeed, cruise altitude, climb profile, range, and required time of arrival (RTA) under wind and departure-time uncertainties have been considered as parameters.

The rest of the paper is organized as follows. In section III, problem formulation for a parametric study of the SOC for the multirotor eVTOL aircraft is presented. In section IV, a parametric study is performed using cruise altitude, cruise airspeed, climb profile, range, and assigned RTA under uncertainties (wind and departure-time) as parameters. Finally, in section V, the main findings from this research study are summarized.

III. Problem Formulation

A. Flight Dynamics and Kinematics Model

In this research, a quadrotor eVTOL aircraft concept proposed by Silva et al. [10], as shown in Figure 1a, is used to perform a parametric study of the SOC of the onboard Li-Po battery pack. A decoupled longitudinal and lateral flight dynamics model (three-dimensional in space and one-dimensional in time) is considered as shown in Figures 1b, 1c and 1d for the trajectory generation. The four lateral states of the model are: $[\lambda, \tau, V_l, \psi]$; where λ is the latitude, τ is the longitude, V_l is the lateral component of the true airspeed and ψ is the heading angle w.r.t north [6, 11, 12]. The two vertical states of the model are: $[h, V_v]$; where h is the altitude and V_v is the vertical component of the true airspeed [3, 11, 12]. The three control variables related to the flight dynamics model are: $[T, \theta, \phi]$; where T is the net thrust, θ is the rotor tip-path-plane pitch angle and ϕ is the rotor tip-path-plane roll (bank) angle. In this research, time derivatives of wind components are assumed to be zero given the short-range operations are expected to be less than 60 miles [1, 2]. Therefore, the quasi-steady flight dynamics and kinematics of the multirotor eVTOL aircraft in a vehicle-carried frame of reference (East-North-Up) are as follows [3, 6, 11]:

$$\frac{dV_l}{dt} = \frac{T\cos\phi\sin\theta - D\cos\gamma}{m} \tag{1}$$

$$\frac{dV_v}{dt} = \frac{T\cos\phi\cos\theta - D\sin\gamma - mg}{m} \tag{2}$$

$$\frac{d\psi}{dt} = \frac{T\sin\phi}{mV_l} \tag{3}$$

$$\frac{d\lambda}{dt} = \frac{V_l\cos\psi + W_n}{(R_{\text{Earth}} + h)} = \frac{V_{GS}\cos\chi}{(R_{\text{Earth}} + h)} \tag{4}$$

$$\frac{d\tau}{dt} = \frac{V_l\sin\psi + W_e}{(R_{\text{Earth}} + h)\cos\lambda} = \frac{V_{GS}\sin\chi}{(R_{\text{Earth}} + h)\cos\lambda} \tag{5}$$

$$\frac{dh}{dt} = V_v + W_v \tag{6}$$

where m is the mass of the eVTOL aircraft, D is the parasite drag, V_{GS} is the groundspeed, χ is the course, h is the altitude above mean sea level, R_{Earth} is the mean radius of the Earth and W_e, W_n and W_v are the components of the wind in east, north and vertical (up) directions, respectively. The aerodynamic flight path angle (γ) is given by:

$$\tan\gamma = \frac{V_v}{V_l} \tag{7}$$

B. Power Balance Model

Power balance equation for a quadrotor eVTOL aircraft is given by [3, 6, 13]:

$$\sum_{i=1}^{n=4} I_i\omega_i\frac{d\omega_i}{dt} = \sum_{i=1}^{n=4} P_i - P_{\text{required}} \tag{8}$$

where P_i is the instantaneous power supplied to the i^{th} rotor by the onboard Li-Po battery pack, P_{required} is the instantaneous power required by the aircraft (to overcome induced drag, profile drag, parasite drag and gravity to climb) [5], ω_i is the rotational speed of the i^{th} rotor, I_i is the rotational moment of inertia of the i^{th} rotor and n is the total number of rotors on a multirotor eVTOL aircraft. In the current research, all four rotors are assumed to be identical with an equal amount of instantaneous power supplied to them. Therefore, the instantaneous total power supplied by the onboard Li-Po battery pack (neglecting transmission losses):

$$P_{\text{battery}} = \sum_{i=1}^{n=4} P_i \tag{9}$$

Hence, the power balance model (Equation: 8) is given by:

$$\frac{d\omega}{dt} = \frac{P_{\text{battery}} - P_{\text{required}}}{4I_{\text{rotor}}\omega} \tag{10}$$

The instantaneous rate of change of rotational speed for each rotor is assumed to be zero based on the following assumptions: i) collective pitch control mechanism is used for the rotor thrust magnitude control and ii) quasi-steady forward flight. Therefore, the power balance (Equation: 8) is given by:

$$P_{\text{battery}} = P_{\text{required}} \tag{11}$$

C. State and Control Vectors

Based on the flight dynamics, flight kinematics, and power balance models, the state vector (X) and control vector (C) to generate trajectories for the eVTOL aircraft are as follows:

$$X = [\lambda\ \tau\ V_l\ \psi\ h\ V_v]^T \tag{12}$$

$$C = [T\ \theta\ \phi]^T \tag{13}$$

D. Thrust Model

The aerodynamic interference between the rotors is assumed to be negligible as the rotors are horizontally separated [5]. The net thrust (T) for the quadrotor eVTOL aircraft is given by [6]:

$$T = 4T_{\text{rotor}} \tag{14}$$

where T_{rotor} is the thrust produced by the isolated rotor and T is net thrust produced by all the rotors.

E. Drag Model

The parasite drag (D) on the multirotor eVTOL is calculated as follows [6, 10]:

$$D = 1.1984\frac{\rho V^2}{2} \tag{15}$$

where ρ is the density of air and V is the true airspeed of the eVTOL aircraft.

F. Power Required

The instantaneous power required in forward flight is equal to the sum of the induced power, parasite power, climb power and profile power as follows [6, 10]:

$$P_{\text{required}} = P_{\text{induced}} + P_{\text{parasite}} + P_{\text{climb}} + P_{\text{profile}} \tag{16}$$

$$P_{\text{required}} = \kappa \sum_{n=1}^{4} (T_{\text{rotor}} v_i)_n + TV \sin\alpha + \frac{\rho A_{\text{rotor}} (\omega R)^3 \sigma C_{d\ mean} F_P}{8} \tag{17}$$

where v_{i} is the induced velocity, κ is the induced power correction factor, α is the angle of attack between the air-stream and the rotor disk (tip-path-plane), V is the true airspeed of the eVTOL aircraft, $C_{\text{d mean}}$ is the mean blade drag coefficient, σ is the thrust weighted solidity ratio and F_{P} is the function that accounts for the increase of the blade section velocity with rotor edgewise and axial speed [6, 10]. The induced velocity (v_{i}) is numerically computed as described in [6].

The $C_{\text{d mean}}$ and κ are functions of the advance ratio (μ). The μ is defined as [5]:

$$\mu = \frac{V\cos\alpha}{\Omega R} \tag{18}$$

G. Path Constraints of the Problem

For a level flight (cruise) in the presence of zero vertical wind, the net vertical force on the multirotor eVTOL aircraft is zero; therefore, the following path constraint is imposed on the problem [6]:

$$T\cos\phi\cos\theta = mg \tag{19}$$

where m is the mass of the multirotor eVTOL aircraft and g is the acceleration due to the gravity.

The path constraint for the great-circle trajectory between the two waypoints is given by [6]:

$$(V_l \sin\psi + W_e)(\sin\lambda_2\cos\lambda_1 - \sin\lambda_1\cos\lambda_2\cos(\tau_2 - \tau_1)) - (V_l\cos\psi + W_n)(\sin(\tau_2 - \tau_1)\cos\lambda_2) = 0 \tag{20}$$

The instantaneous power required (Equation: 17) is bounded by the total maximum available power to the four rotors in kW [5, 10]:

$$P_{\text{required}} \leq 494.25 \tag{21}$$

H. Battery Models

1. Energy-Based Model (Battery Model 1)

For an electric aircraft, the onboard Li-Po battery pack is equivalent to the fuel tank system for which the fuel quantity stored and burned is measured in energy (Mega-Joules) [5]. The maximum usable capacity (E_{cap}) of the onboard Li-Po battery pack for the eVTOL aircraft considered in this research is 1331 MJ [10]. The E_{cap} accounts for

efficiency and losses in the electric fuel system. As stated earlier, in this research, the mechanical losses are ignored (Equation: 11), as the main goal is to get a qualitative understanding of the effect of various flight parameters on the state of the onboard Li-Po battery pack. Therefore, the energy consumption (E_{con}) from the Li-Po battery pack is considered equal to the energy consumption by the rotor blades to overcome induced drag, parasite drag, profile drag, and gravity during the flight. In model 1, the state of charge (SOC) of a battery is defined as 1 when the battery has the maximum usable energy, i.e., E_{cap} and 0 when the battery has zero usable energy ,i.e., the SOC represents battery pack's remaining deliverable capacity. To perform parametric studies and understand the impact of various flight parameters on the usage of the onboard Li-Po battery pack, the SOC is predicted as follows [5]:

$$SOC = \begin{cases} 0, & \text{if } 1 < \frac{E_{\text{con}}}{E_{\text{cap}}}; \\ 1 - \frac{E_{\text{con}}}{E_{\text{cap}}}, & \text{if } \frac{E_{\text{con}}}{E_{\text{cap}}} \leq 1; \end{cases}$$

2. Electrochemical-Based Model (Battery Model 2)

The second battery model used in this research is the electrochemical-based model of Li-Po battery pack developed by Daigle, M., and Kulkarni, C [4]. This model captures the significant electrochemical processes, and it reliably predicts state of charge (SOC) and end-of-discharge (EOD). The discharging process consists of three discharging zones, i.e., exponential zone, nominal zone, and fast-discharging zone in electrochemical-based model [4]. This model and prognostics algorithms have been verified and validated on electric UAVs in earlier research work [14].

Theoretically each cell has a voltage of around 4.2V when fully charged. The terminal voltage of the battery rises/falls based on the charge/discharge, this settles to a steady stage voltage at the end of the respective cycle, which is a function of its state of charge (SOC). SOC is conventionally defined to be 1 when the battery is completely charged to 4.2V and 0 when the battery is fully discharged.

In this model, the SOC is analogous to the mole fraction x_n, but scaled from 0 to 1. There is a difference here between nominal SOC and *apparent* SOC. Nominal SOC is computed based on the combination of the bulk and surface layer control volumes i.e. number of ions in the negative electrode, whereas apparent SOC would be computed based only on the surface layer [4]. That is, a battery can be discharged at a given rate and reach the pre-defined voltage cutoff, i.e., apparent SOC is then 0.

Nominal (n) and apparent (a) SOC can then be defined using

$$SOC_n = \frac{q_n}{0.6q^{\max}} \tag{22}$$

$$SOC_a = \frac{q_{s,n}}{0.6q^{\max_{s,n}}}, \tag{23}$$

where $q^{\max_{s,n}} = q^{\max}\frac{v_{s,n}}{v_n}$. The factor $1/0.6$ comes from the fact that the mole fraction at the positive electrode cannot go below 0.4, therefore SOC of 1 corresponds to the point where $q_n = 0.6q^{\max_{s,n}}$.

In this work the flight profile of 43 m/s at 30 nm is considered a nominal operational flight with a load of 0.6C rate on the battery pack [10]. The power consumed of 144 kW by the vehicle at these requirements is then normalized with the rest of the flight profiles under study and to a single cell in a battery pack. The model is generalized for different battery pack sizes and can be modified with additional information of the pack size for future studies.

In order to predict end-of-discharge as defined by a set voltage cutoff, i.e, apparent SOC value, the battery model must compute the voltage as a function of time given the current drawn from the battery. The developed model in this work specifically on Li-ion 18650 batteries with an average nominal voltage of 3.7V and nominal capacity of 2200mAh, however, the model is still general enough that with some modifications it may be applied to different battery chemistry types [4].

IV. Parametric Study and Results

A. Trajectory Generator

In this research, for a parametric study of the SOC, great-circle trajectories are generated using the point mass model (Equations: 1 - 6) and great-circle navigation law (Equation: 20) that employs thrust (T), rotor tip-path-plane pitch (θ) and bank (ϕ) angles as controls. The equations of motion are integrated forward in time using the controls needed for following the desired lateral path (great-circle) and vertical path (climb, and cruise) [15]. The energy consumption and SOC depletion for the flight plan are computed using the power and battery models, as shown in Figure 2.

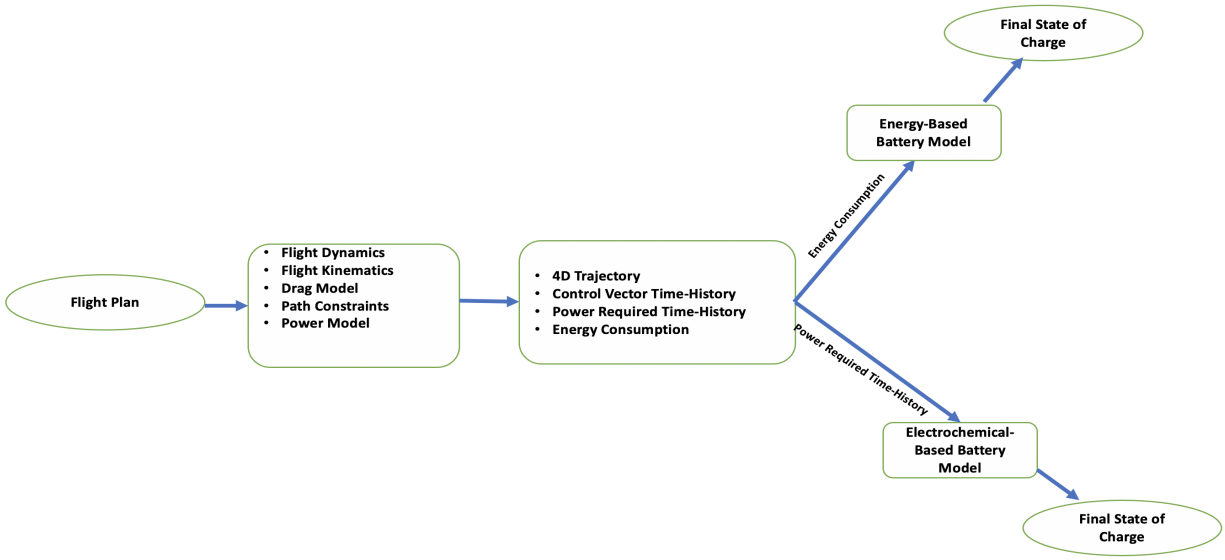

Fig. 2 Energy consumption and final SOC computations

B. Performance Data

Table 1 shows performance data of the eVTOL aircraft used in this research for the parametric study [5, 10]. The thrust coefficient (C_{T}) is approximated as a constant assuming collective pitch control mechanism used for the rotor thrust magnitude control [5].

Table 1 Performance data of the eVTOL aircraft

Parameter (Unit)	Value
V_{MO}	109 kts (56 m/s)
R	4.0 m
A_{rotor}	50.26 m^2
mass	2940 kg
σ	0.055
F_{P}	0.97
C_{T}	0.0055

Based on the induced power correction factor (κ) and mean blade drag coefficient ($C_{\mathrm{d\ mean}}$) data [5] as a function of advance ratio (μ is defined in Equation: 24), for the eVTOL aircraft in forward flight, κ and $C_{\mathrm{d\ mean}}$ are approximated as follows:

$$\kappa = 1.09 - 0.20\mu + 1.23\mu^2 + 28.40\mu^3 \tag{24}$$

$$C_{d\ mean} = 0.0085 + 0.0121\mu - 0.1074\mu^2 + 0.3182\mu^3 \tag{25}$$

C. Case Study I - Cruise Airspeed, Range and Cruise Altitude

1. Minimum-Energy Cruise Airspeed

The energy consumption (MJ), the power required (kW), and final SOC (energy-based and electrochemical-based) to cruise 100 nm at different constant cruise airspeeds between 20 m/s (38.87 kts) and 60 m/s (116.63 kts); and different

cruise altitudes above MSL: [500 m (1640 ft), 1000 m (3280 ft), 2000 m (6561 ft), 3000 m (9842 ft)] are shown in Figure 3. For this parametric study, as stated the parameter cruise airspeed is varied from 20 m/s to 60 m/s in steps of 5 m/s for a chosen cruise altitude. First, the cruise airspeed with the minimum-energy consumption is identified for a given cruise altitude. Next, the cruise airspeed is further varied in steps of 1 m/s around the previously found minimum-energy cruise airspeed to find a more accurate cruise airspeed value with minimum-energy consumption. In addition, the initial value of the SOC at the top of climb is assumed to be 1. From Figure 3a, Figure 3b and Table 2, it can be observed that the value of the minimum-energy cruise airspeed (maximum final SOC) increases with an increase in cruise altitude. The minimum-energy cruise airspeed (93.3 kts) at 3000 m MSL computed in this research (Table 2) is within 5 % margin of the long-range cruise airspeed (98 kts) computed at 3000 m MSL for the eVTOL aircraft in [10]. In general, the long-range cruise airspeed is 3 - 5 % faster than the best-range airspeed.

Results (Figure 3c), using energy-based battery model, show that flying cruise segment of 100 nm at constant cruise airspeed slower than 20 m/s is infeasible. However, results (Figure 3d), using the electrochemical-based battery model, show lower final SOC compared to the energy-based model at the end of the cruise segment. Figure 3d also shows i) flying at constant cruise airspeed slower than 30 m/s is infeasible for the chosen eVTOL aircraft, and ii) slight advantage in terms of battery usage flying near the maximum operating limit airspeed (V_{MO}) at higher cruise altitudes because of lower parasite drag and profile drag.

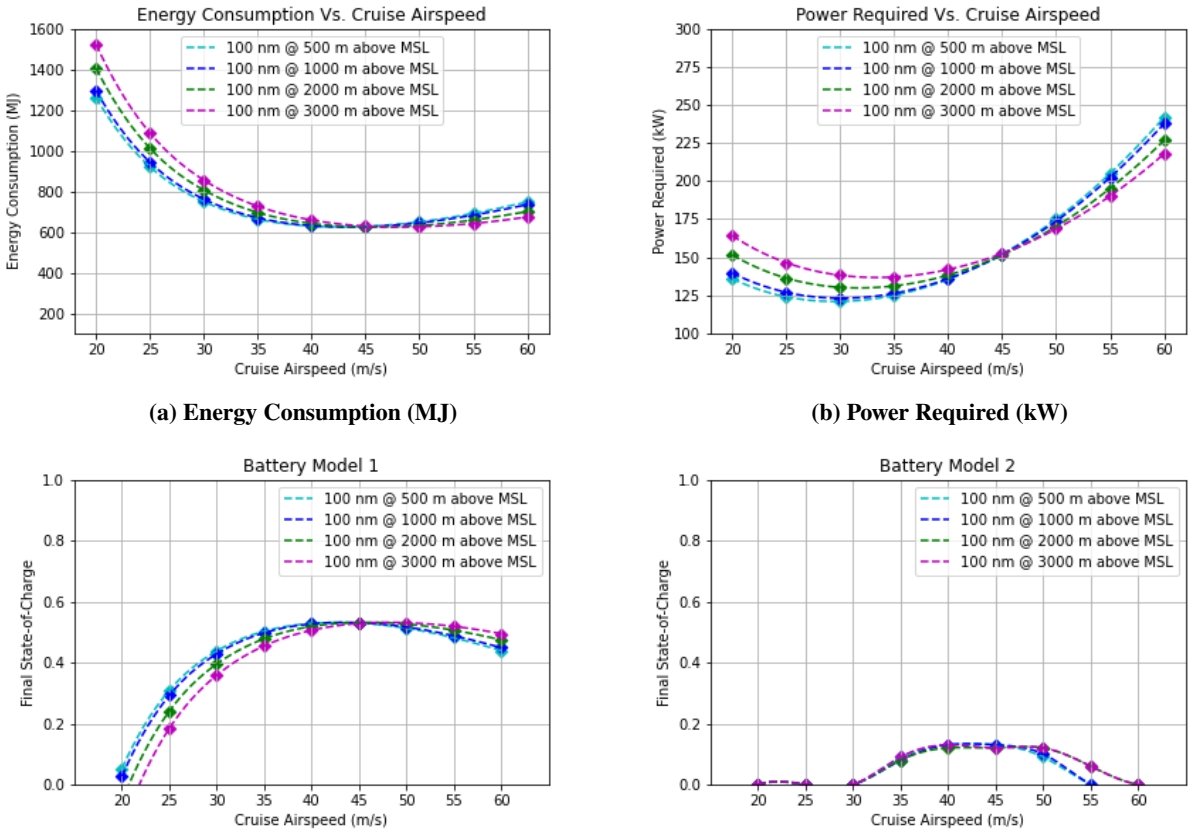

(a) Energy Consumption (MJ)

(b) Power Required (kW)

(c) Final SOC (Battery Model 1)

(d) Final SOC (Battery Model 2)

Fig. 3 Energy consumption, power required and final SOC (battery model 1 and battery model 2) for 100 nm cruise segment at different cruise airspeeds and cruise altitudes

2. Range

For this case study, the range is used as the variable parameter. The initial value of the SOC at the top of climb is assumed to be 1. From Figure 4, it can be observed that, irrespective of cruise segment length (100 nm, 70 nm, 50 nm, and 30 nm), the minimum-energy (maximum final SOC) cruise airspeed is ~ 43 m/s at 500 m MSL, i.e., independent of

Table 2 Minimum-energy cruise airspeed

Cruise Altitude (MSL)	Cruise Airspeed
500 m (1640 ft)	43 m/s (83.6 kts)
1000 m (3280 ft)	44 m/s (85.5 kts)
2000 m (6561 ft)	46 m/s (89.4 kts)
3000 m (9842 ft)	48 m/s (93.3 kts)

the length of the cruise segment. Figure 4b shows low final SOC values for 100 nm cruise segment irrespective of the cruise airspeed. This behavior can be attributed to differences between the discharge characteristics of the two models described in [5] and [4].

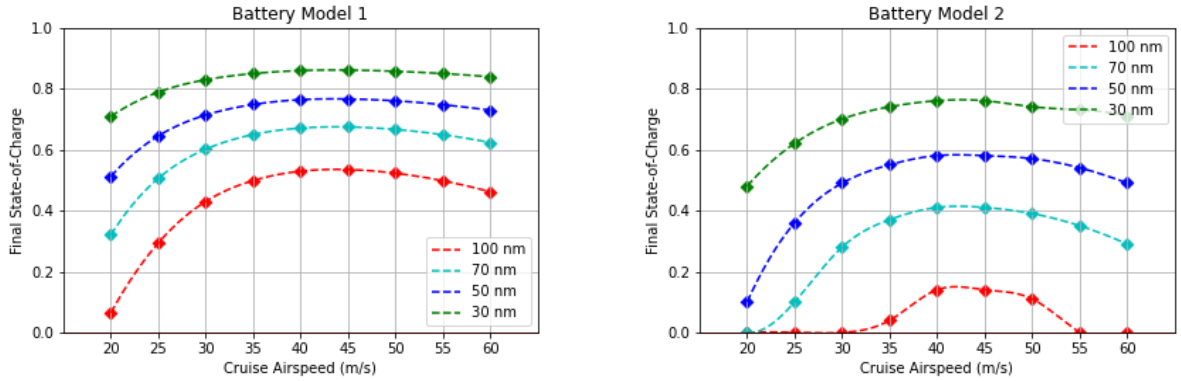

(a) Final SOC (Battery Model 1) **(b) Final SOC (Battery Model 2)**

Fig. 4 Final SOC (battery model 1 and battery model 2) for different cruise segments and cruise airspeeds at fixed cruise altitude of 500 m above MSL

3. Climb and Cruise Segments

The climb flight procedure of the eVTOL aircraft is assumed to be as follows: i) an initial climb vertically to 15 m (50 ft) AGL, ii) climb at a 10-degree flight path angle at the forward speed of 30 m/s (approximate minimum power cruise airspeed) [10], iii) the transition phase to level off at the cruise altitude at the best-range cruise airspeed, and iv) constant length cruise segment (30 nm or 100 nm). For the parametric study of the SOC, the initial value of the SOC, i.e., at the start of the climb segment (15 m AGL), is assumed to be 1. From Figure 5, it can be observed that irrespective of the range, flying at a lower cruise altitude is beneficial in terms of energy consumption and battery usage. Therefore, from an energy consumption and battery usage perspective, designing a cruise corridor for urban air mobility air traffic is suggested at the lowest altitude where: i) eddies/vortices from the buildings are minimal, ii) vertical obstacles are avoided with a safety margin, and iii) interactions of UAM air traffic with other types of air traffic (UTM and commercial) is minimal. Also, comparing Figure 5c with Figure 5d, it can be observed that the final SOC prediction using the electrochemical-based model is lower than the energy-based model for the 100 nm cruise segment. This behavior can be attributed to differences between the discharge characteristics of the two models described in [5] and [4].

D. Case Study II - Required Time of Arrival Under Uncertainties

One way to achieve a controlled UAM traffic flow to the vertiport is by assigning arrival constraints at selected waypoints (metering fixes) that aircraft must meet using an onboard control system for dynamic airspeed adjustment. This procedure is often characterized as the required time of arrival (RTA) [3]. Similarly, to maintain the minimum spatial separation between flights on two separate routes crossing a common waypoint at the same altitude under high

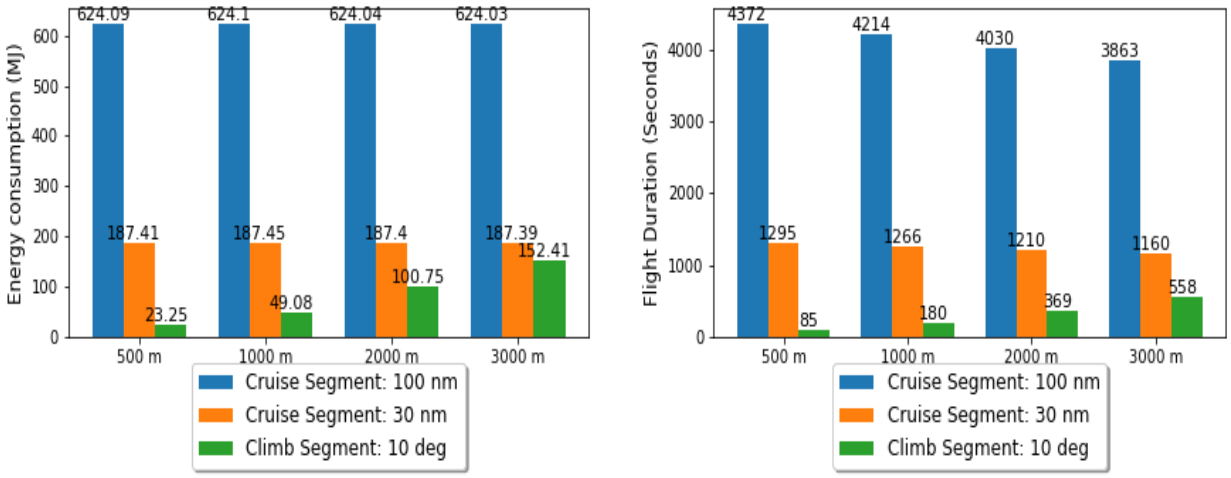

(a) Energy Consumption (MJ)

(b) Flight Duration (Seconds)

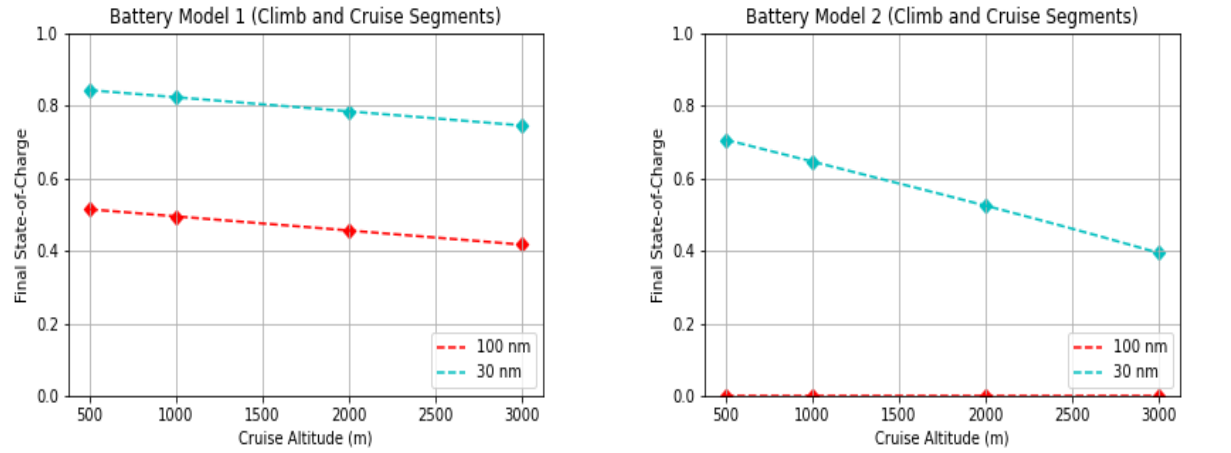

(c) Final SOC (Battery Model 1)

(d) Final SOC (Battery Model 2)

Fig. 5 Energy consumption, flight duration and final SOC (battery model 1 and battery model 2) for 100 nm and 30 nm cruise segments at the minimum-energy cruise airspeed with climb to different cruise altitudes at 10-deg flight path angle

traffic density, the flights may be required to cross the waypoint at a precise time. Therefore, in order to study the impact of assigning RTA on energy consumption and SOC, two metering fixes that are 30 nm and 100 nm away from the eVTOL aircraft in the cruise phase at an altitude of 500 m MSL are considered.

1. Wind Magnitude Uncertainty

In this parametric study, the wind is assumed to be uniform, i.e., constant magnitude and direction. Therefore, the impact of wind magnitude uncertainty (actual wind magnitude - predicted wind magnitude) on the SOC of the onboard Li-Po battery pack is studied. The RTA at the metering fix (30 nm away from the aircraft) is assumed to be assigned by a scheduler based on the predicted wind and nominal cruise airspeed of the eVTOL aircraft (Table 2). Figure 6 and Table 3 show that based on the wind direction relative to the route, wind magnitude, and wind magnitude uncertainty, requiring an aircraft to meet an assigned RTA will have an impact on its battery usage. The eVTOL aircraft may consume more or less of the battery than predicted by the fleet operator for the UAM trip. Therefore, wind magnitude uncertainty could directly impact fleet planning. Similar trend is observed for the impact of wind magnitude uncertainty on the final SOC prediction at a cruise altitude of 3000 m MSL.

Table 3 Flight duration, energy consumption and final SOC without wind uncertainty

Metering Fix (nm)	Wind (kts)	Flight Duration (sec)	Energy Consumption (MJ)	Final SOC (Battery Model 1)	Final SOC (Battery Model 2)
30	Headwind: 26	1879	272.3	0.7953	0.639
30	Tailwind: 26	987	142.9	0.8591	0.812

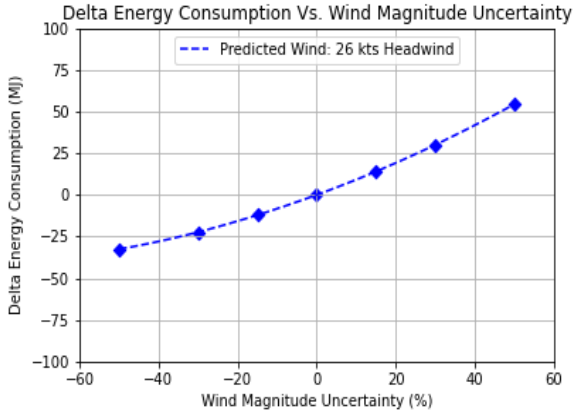

(a) Headwind 26 kts: Delta Energy consumption (MJ)

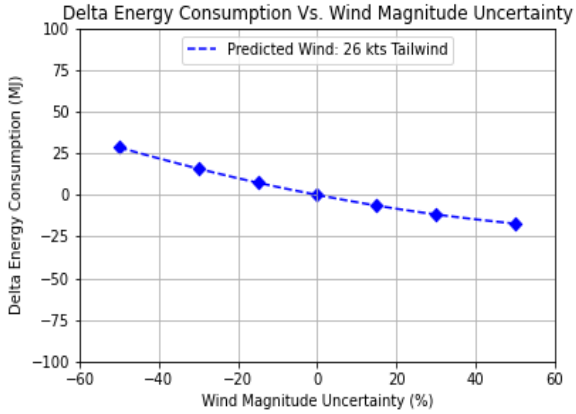

(b) Tailwind 26 kts: Delta Energy consumption (MJ)

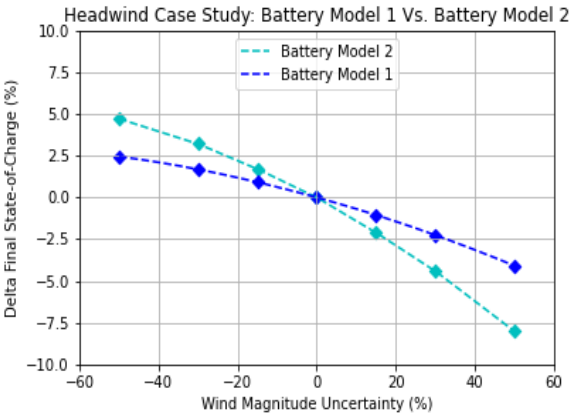

(c) Headwind 26 kts: Delta Final SOC (%)

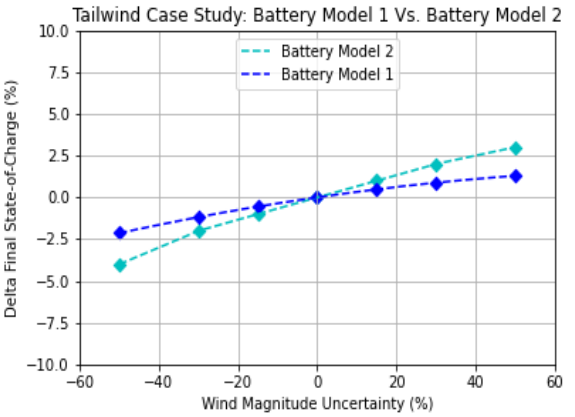

(d) Tailwind 26 kts: Delta Final SOC (%)

Fig. 6 Delta energy consumption and delta battery usage (model 1 and model 2) while flying to meet an assigned RTA under various values of wind magnitude uncertainty

2. Departure-Time Uncertainty

In this parametric study, the impact of departure-time uncertainty on the SOC of the onboard Li-Po battery pack is studied. The uncertainty in the departure-time from the scheduled time of departure (STD) in the on-demand UAM could stem from many reasons such as takeoff pad constraint, delay in passenger loading, maintenance actions, etc. However, given the constraint on arrival vertiport infrastructure, the eVTOL aircraft may still need to meet the assigned RTA either by speeding up or slowing down in the cruise phase [3]. The RTA at the metering fix is assumed to be assigned by a scheduler based on the STD and nominal cruise airspeed (Table 2). From Figure 7, it can be observed that closer the metering fix to the eVTOL aircraft, the larger would be the adverse impact (nonlinear) of departure-time uncertainty on the energy consumption and battery usage. Figure 7b (electrochemical-based model) shows higher adverse impact of the departure-time uncertainty on the usage of the onboard Li-Po battery pack in the time-controlled air traffic flow environment. Similar trend is observed for the impact of departure-time uncertainty on the final SOC prediction at a cruise altitude of 3000 m MSL.

Table 4 Flight duration, energy consumption and final SOC without departure-time uncertainty

Metering Fix (nm)	Flight Duration (sec)	Energy Consumption (MJ)	Final SOC (Battery Model 1)	Final SOC (Battery Model 2)
30	1294	187.41	0.8591	0.755
100	4312	624.09	0.5311	0.139

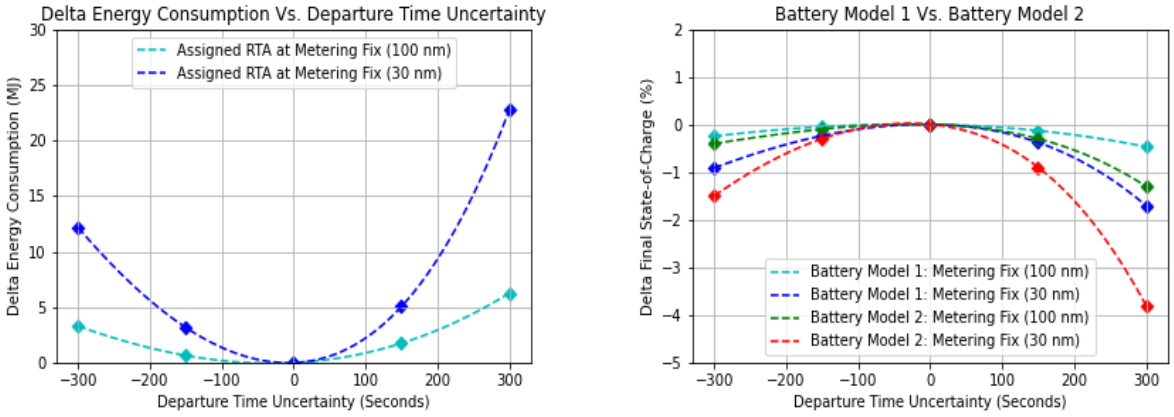

(a) Delta Energy consumption (MJ) **(b) Delta Final SOC (%)**

Fig. 7 Delta energy consumption and delta battery usage (model 1 and model 2) while flying to meet an assigned RTA under various departure-time uncertainty

V. Conclusion

In this research, a parametric study of the state of charge is performed using two separate battery models, i.e., energy-based and electrochemical-based battery models for a NASA-proposed conceptual multirotor aircraft flight in the urban environment. The parameters considered for the parametric analysis are cruise airspeed, cruise altitude, climb profile, range, and required time of arrival under wind and departure-time uncertainties. The parametric study showed: i) the minimum-energy cruise airspeed (maximum final state of charge) increases with an increase in cruise altitude; ii) the minimum-energy cruise airspeed is independent of range; iii) from an energy consumption perspective, designing a cruise corridor for urban air mobility air traffic is suggested at the lowest possible altitude where eddies/vortices from the skyscrapers in the metroplex are minimal; iv) wind and departure-time uncertainties could adversely impact the predictability of the usage of the onboard lithium-ion polymer battery pack for an aircraft flying to meet the assigned required time of arrival in the urban air mobility environment. The state of charge results showed high dependence on

the battery model.

In conclusion, this study demonstrates the need for urban air mobility fleet operators to: i) plan and fly minimum-energy trajectories given low-specific energy of lithium-ion polymer battery pack, and ii) have a validated battery model for the onboard lithium-ion polymer battery pack to predict the state of charge accurately.

Acknowledgments

The authors thank Dr. Heinz Erzberger, Dr. Wayne Johnson, Christopher Silva, Andrew Cone and Dr. Thomas Lombaerts from NASA Ames Research Center for discussions, reviews and helpful suggestions. The material is based upon work supported by NASA under award number NNA16BD14C for NASA Academic Mission Services (NAMS).

References

[1] Uber-Elevate, "Fast-forwarding to the future of on-demand, urban air transportation," `https://www.uber.com/`, 2019. [Online; accessed 19-June-2019].

[2] Thipphavong, D. P., Apaza, R., Barmore, B., Battiste, V., Burian, B., Dao, Q., Feary, M., Go, S., Goodrich, H. J., Kenneth H, Idris, H. R., Kopardekar, P. H., Lachter, J. B., Neogi, N. A., Ng, H. K., Oseguera-Lohr, R. M., Patterson, M. D., and Verma, S. A., "Urban air mobility airspace integration concepts and considerations," *2018 Aviation Technology, Integration, and Operations Conference*, 2018, p. 3676. doi:10.2514/6.2018-3676.

[3] Pradeep, P., and Wei, P., "Energy-efficient arrival with rta constraint for multirotor evtol in urban air mobility," *Journal of Aerospace Information Systems*, Vol. 16, No. 7, 2019, pp. 263–277.

[4] Daigle, M., and Kulkarni, C., "Electrochemistry-based Battery Modeling for Prognostics," *Annual Conference of the Prognostics and Health Management Society 2013*, 2013, pp. 249–261.

[5] Johnson, W., "NDARC-NASA Design and Analysis of Rotorcraft," 2015.

[6] Pradeep, P., Lauderdale, T. A., Chatterji, G. B., Sheth, K., Lai, C. F., Sridhar, B., Edholm, K.-M., and Erzberger, H., "Wind-Optimal Trajectories for Multirotor eVTOL Aircraft on UAM Missions," *AIAA AVIATION 2020 FORUM*, 2020, p. 3271.

[7] Falck, R. D., Chin, J., Schnulo, S. L., Burt, J. M., and Gray, J. S., "Trajectory optimization of electric aircraft subject to subsystem thermal constraints," *18th AIAA/ISSMO Multidisciplinary Analysis and Optimization Conference*, 2017, p. 4002.

[8] Chauhan, S. S., and Martins, J. R., "Tilt-wing eVTOL takeoff trajectory optimization," *Journal of Aircraft*, Vol. 57, No. 1, 2020, pp. 93–112.

[9] "Uber Air Vehicle Requirements and Missions," , 2020. URL `https://s3.amazonaws.com/uber-static/elevate/SummaryMissionandRequirements.pdf`, [Online; accessed 16-April-2020].

[10] Silva, C., Johnson, W. R., Solis, E., Patterson, M. D., and Antcliff, K. R., "VTOL Urban Air Mobility Concept Vehicles for Technology Development," *2018 Aviation Technology, Integration, and Operations Conference*, 2018, p. 3847.

[11] Yomchinda, T., Horn, J., and Langelaan, J., "Flight path planning for descent-phase helicopter autorotation," *AIAA Guidance, Navigation, and Control Conference*, 2011, p. 6601.

[12] Tsuchiya, T., Ishii, H., Uchida, J., Ikaida, H., Gomi, H., Matayoshi, N., and Okuno, Y., "Flight trajectory optimization to minimize ground noise in helicopter landing approach," *Journal of guidance, control, and dynamics*, Vol. 32, No. 2, 2009, pp. 605–615.

[13] Johnson, W., *Helicopter theory*, Courier Corporation, 2012.

[14] Hogge, E., Bole, B., Vazquez, S., Kulkarni, C., Strom, T., Hill, B., Smalling, K., and Quach, C., "Verification of Prognostic Algorithms to Predict Remaining Flying Time for Electric Unmanned Vehicles," *International Journal of Prognostics and Health Management, ISSN 2153-2648, 2018 021*, 2018.

[15] Becerra, V. M., "Solving complex optimal control problems at no cost with PSOPT," *2010 IEEE International Symposium on Computer-Aided Control System Design*, 2010, pp. 1391–1396. doi:10.1109/CACSD.2010.5612676.